Mouse TEX15 is essential for DNA double-strand break repair and chromosomal synapsis during male meiosis

Fang Yang,[1] Sigrid Eckardt,[2] N. Adrian Leu,[2] K. John McLaughlin,[2] and Peijing Jeremy Wang[1]

[1]Department of Animal Biology, School of Veterinary Medicine, University of Pennsylvania, Philadelphia, PA 19104
[2]Center for Animal Transgenesis and Germ Cell Research, New Bolton Center, University of Pennsylvania, Kennett Square, PA 19348

During meiosis, homologous chromosomes undergo synapsis and recombination. We identify TEX15 as a novel protein that is required for chromosomal synapsis and meiotic recombination. Loss of TEX15 function in mice causes early meiotic arrest in males but not in females. Specifically, TEX15-deficient spermatocytes exhibit a failure in chromosomal synapsis. In mutant spermatocytes, DNA double-strand breaks (DSBs) are formed, but localization of the recombination proteins RAD51 and DMC1 to meiotic chromosomes is severely impaired. Based on these data, we propose that TEX15 regulates the loading of DNA repair proteins onto sites of DSBs and, thus, its absence causes a failure in meiotic recombination.

Introduction

Homologous recombination allows the reciprocal exchange of genetic material between parental genomes and ensures proper chromosome segregation during the first meiotic cell division (Zickler and Kleckner, 1999). Meiotic recombination is initiated by the generation of DNA double-strand breaks (DSBs; Keeney, 2001). In eukaryotes, DSB formation depends on the SPO11 protein (Keeney et al., 1997; Baudat et al., 2000; Romanienko and Camerini-Otero, 2000). Generation of DSBs causes a DNA damage response, which is accompanied by the phosphorylation of histone variant H2AX (γH2AX; Mahadevaiah et al., 2001). DSBs are resected to generate 3′ single-stranded overhangs, and DNA repair proteins, such as RAD51 and DMC1, load onto single-stranded DNA (ssDNA), forming foci at DSB sites (Tarsounas et al., 1999). The ssDNA then invades the homologous chromosome, which leads to the formation of double Holliday junctions that are resolved as either crossovers or noncrossovers (Hunter and Kleckner, 2001).

The recruitment of RAD51 and DMC1 to meiotic chromosomes is critical for DSB repair (Bannister and Schimenti, 2004; Marcon and Moens, 2005). DMC1, a meiosis-specific homologue of RAD51, forms a complex with RAD51 (Bishop et al., 1992; Tarsounas et al., 1999). Breast cancer susceptibility gene products BRCA1 and 2 have also been found to participate in early steps of meiotic recombination in higher eukaryotes. BRCA1 and 2 are associated with RAD51 in both mitotic and meiotic cells (Scully et al., 1997; Davies et al., 2001). In *Brca1* mutant spermatocytes, RAD51, but not DMC1, foci are reduced (Xu et al., 2003). In *Brca2* mutant spermatocytes, both RAD51 and DMC1 foci are dramatically decreased (Sharan et al., 2004; Cotroneo et al., 2007). Therefore, mutations in either *Brca1* or *2* cause a failure in meiotic recombination.

Although the process of meiotic recombination is highly conserved among different species, species-specific meiosis proteins have evolved (Marcon and Moens, 2005). For example, MEI1, a vertebrate-specific meiosis factor, appears to function in the generation of DSBs (Libby et al., 2003). A previous systematic genomic screen has identified 36 germ cell–specific genes that are expressed in mouse spermatogonia (Wang et al., 2001). Some of these genes have been disrupted in mice and the majority of these mutants display defects in meiosis (Wang and Pan, 2007). In this paper, we report the functional characterization of one of these genes, *Tex15*, and demonstrate that mouse TEX15 is required for DSB repair and chromosomal synapsis in males.

Results and discussion

Tex15 is required for male meiosis

Mouse TEX15 is a 2,785-aa serine-rich protein with no known function motifs (Wang et al., 2001). Database searches reveal that *Tex15* orthologues are present in mammals and zebrafish.

Correspondence to Peijing Jeremy Wang: pwang@vet.upenn.edu

Abbreviations used in this paper: DSB, double-strand break; ES, embryonic stem; RPA, replication protein A; SC, synaptonemal complex; ssDNA, single-strand DNA.

The online version of this paper contains supplemental material.

The Journal of Cell Biology, Vol. 180, No. 4, February 25, 2008 673–679
http://www.jcb.org/cgi/doi/10.1083/jcb.200709057

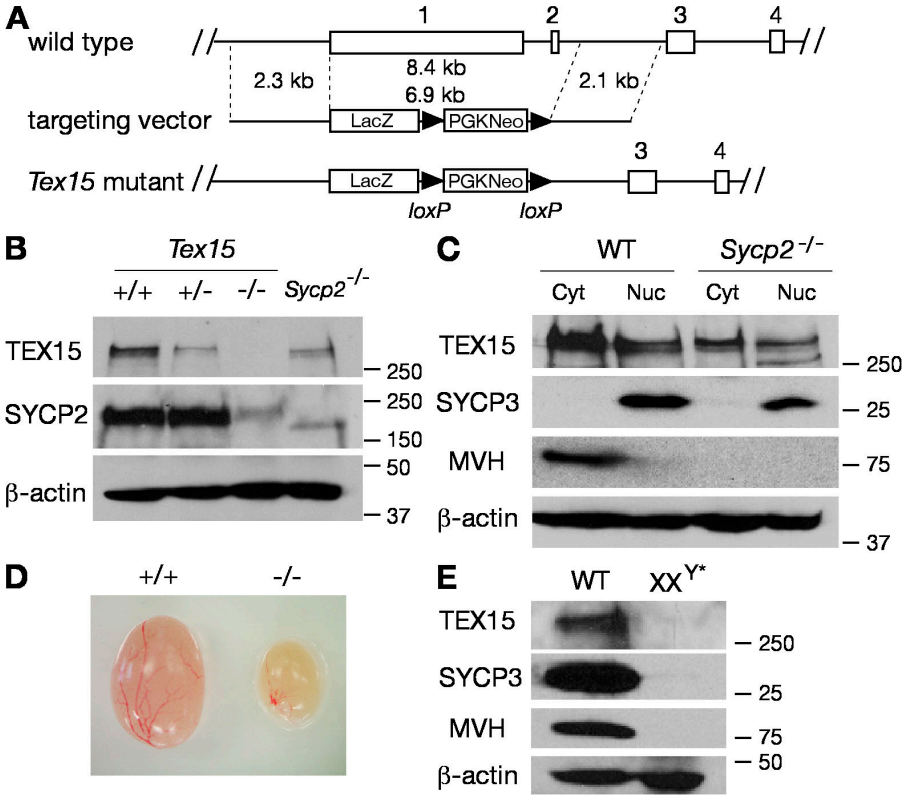

Figure 1. **Targeted inactivation of the *Tex15* gene.** (A) Schematic diagram of the *Tex15* targeting strategy. The four exons of *Tex15* are drawn in scale as rectangles and are designated by the numbers shown above. The neomycin selection marker is flanked by *loxP* sites and the orientation of *loxP* sites is indicated by arrowheads. The *LacZ* coding sequence is preceded by an IRES sequence and followed by SV40 polyadenylation signal sequence (not depicted). (B) Absence of TEX15 protein in *Tex15*$^{-/-}$ testes. Western blot analysis was performed on 20 µg each of adult wild-type, *Tex15*$^{+/-}$, *Tex15*$^{-/-}$, and *Sycp2*$^{-/-}$ testicular protein extracts. SYCP2 served as a nuclear protein control. (C) TEX15 is present in both the cytoplasm and nucleus in testes. Cytoplasmic (Cyt) and nuclear (Nuc) fractions were prepared from adult wild-type and *Sycp2*$^{-/-}$ testes. MVH, predominantly expressed in spermatocytes and spermatids, served as a cytoplasmic protein control (Toyooka et al., 2000). SYCP3 served as a nuclear protein control. (D) Dramatic size reduction in *Tex15*$^{-/-}$ testis. (E) Absence of TEX15 in germ cell–deficient XX^{Y*} testis. 30 µg of total testicular protein extracts from adult wild-type (WT) or germ cell–deficient (XX^{Y*}) testes were used for Western blot analysis with antibodies against indicated proteins (Hunt and Eicher, 1991). Protein molecular mass standards are shown in kilodaltons (B, C, and E).

However, *Tex15* has no apparent sequence homologues in yeast, worms, flies, or chicken. The expression of *Tex15* is dynamic throughout spermatogenesis. *Tex15* transcript is present in spermatogonia and early spermatocytes, is down-regulated in pachytene spermatocytes, and is abundant in postmeiotic germ cells, indicating that *Tex15* might function at different developmental stages during spermatogenesis (Wang et al., 2005). To elucidate its putative function in spermatogenesis, we disrupted the *Tex15* gene by homologous recombination in embryonic stem (ES) cells. Sequence analysis revealed that the mouse *Tex15* gene consists of four exons and spans a genomic region of 15 kb on chromosome 8. In the targeting construct, 8.4-kb genomic DNA harboring the first two exons was replaced with a *LacZ*-neomycin selection cassette (Fig. 1 A). Deletion of the first two exons (7.1 kb and 50 bp, respectively), accounting for 85% of the coding region, was expected to disrupt the *Tex15* gene.

Tex15$^{-/-}$ mice were viable and no overt defects were observed at up to 8 mo of age. Interbreeding of heterozygous (*Tex15*$^{+/-}$) mice yielded a normal Mendelian ratio (17:37:15) of *Tex15*$^{+/+}$, *Tex15*$^{+/-}$, and *Tex15*$^{-/-}$ offspring. However, the fertility phenotype of *Tex15*$^{-/-}$ mice was sexually dimorphic. *Tex15*$^{-/-}$ males were sterile, whereas *Tex15*$^{-/-}$ females were fertile. Western blot analysis demonstrated absence of the full-length TEX15 protein in *Tex15*$^{-/-}$ testes (Fig. 1 B). However, it cannot be excluded that the C-terminal portion of TEX15, encoded by exons 3 and 4, may be present. In wild-type testes, TEX15 protein is present in both the cytoplasm and nucleus (Fig. 1 C). TEX15 is also detected in testes from *Sycp2* mutant mice (Fig. 1, B and C), in which meiosis is arrested at the zygotene stage (Yang et al., 2006), showing that the TEX15 protein is present in early spermatocytes. In addition, the reduced level of TEX15 in the *Sycp2* mutant testes suggests that TEX15 is abundant in germ cells of later stages that are absent in the *Sycp2* mutant.

Disruption of *Tex15* resulted in dramatically reduced testis size (Fig. 1 D). The weight of *Tex15*$^{-/-}$ testes (31.3 ± 1.8 mg/pair; $P < 0.0026$) from 2-mo-old mice was <20% that of *Tex15*$^{+/-}$ testes (174.2 ± 43.6 mg/pair). The testes of sterile XX^{Y*} male mice are completely devoid of germ cells but contain somatic cells such as Sertoli and Leydig cells (Hunt and Eicher, 1991). The absence of TEX15 in XX^{Y*} testes (Fig. 1 E) demonstrates that expression of TEX15 is germ cell specific. This suggests that the sterility of *Tex15*-deficient males is caused by a germ cell–intrinsic defect rather than indirectly by somatic cell defects.

In contrast to wild-type seminiferous tubules with a full spectrum of spermatogenic cells (Fig. 2 A), seminiferous tubules from adult *Tex15*$^{-/-}$ testes exhibited a complete lack of pachytene spermatocytes and postmeiotic germ cells, indicating early meiotic arrest (Fig. 2, B–D). Consistent with this, epididymal tubules from *Tex15*$^{-/-}$ mice were depleted of germ cells (Fig. 2 F). Seminiferous tubules in *Tex15*$^{-/-}$ testes contained two to three layers of darkly stained zygotene-like germ cells (Fig. 2 B). In some tubules, apparently abnormal cells with enlarged nuclei presumably corresponded to apoptotic germ cells (Fig. 2 C). TUNEL analysis revealed dramatically increased apoptosis in *Tex15*$^{-/-}$ testes compared with the wild type (unpublished data). We also detected tubules with a single layer of early spermatogenic/Sertoli cells (Fig. 2 D). As spermatogenesis is synchronous in each given tubule, this heterogeneity reflects various stages of failed germ cell development as a result of meiotic arrest caused by disruption of *Tex15*. To narrow down the point of

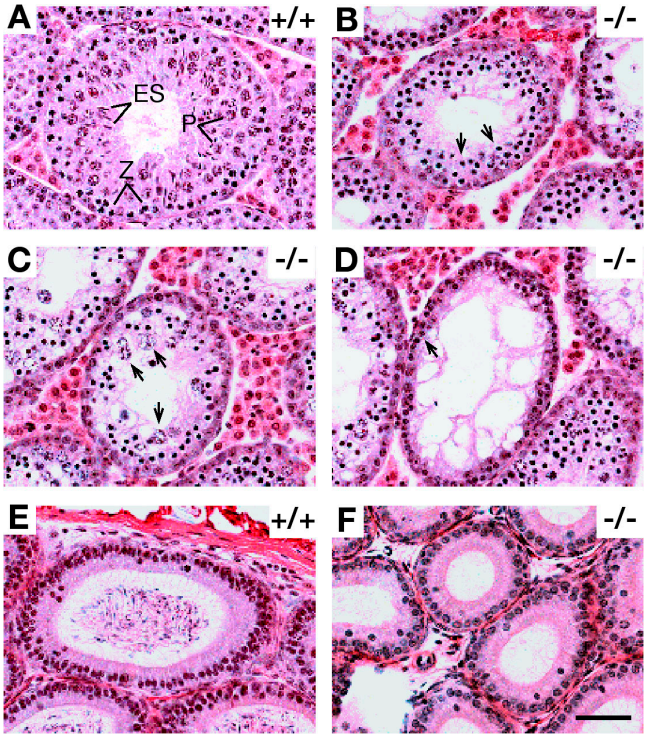

Figure 2. **Meiotic arrest in *Tex15*-deficient mice.** Testes and epididymides from 7-wk wild-type and *Tex15*$^{-/-}$ mice were subject to histological analysis. (A) A wild-type seminiferous tubule contains a full spectrum of germ cells: zygotene spermatocytes (Z), pachytene spermatocytes (P), and elongating spermatids (ES). (B) In some *Tex15*$^{-/-}$ seminiferous tubules, two to three layers of zygotene-like spermatocytes (arrows) are present. (C) *Tex15*$^{-/-}$ tubules with large but lightly stained degenerating spermatocytes (arrows). (D) *Tex15*$^{-/-}$ tubules with only a single layer of early spermatogenic and Sertoli cells (arrow). (E) Wild-type epididymal tubules were full of spermatozoa. (F) Epididymal tubules from *Tex15*$^{-/-}$ mice were devoid of germ cells. Bar, 50 µm.

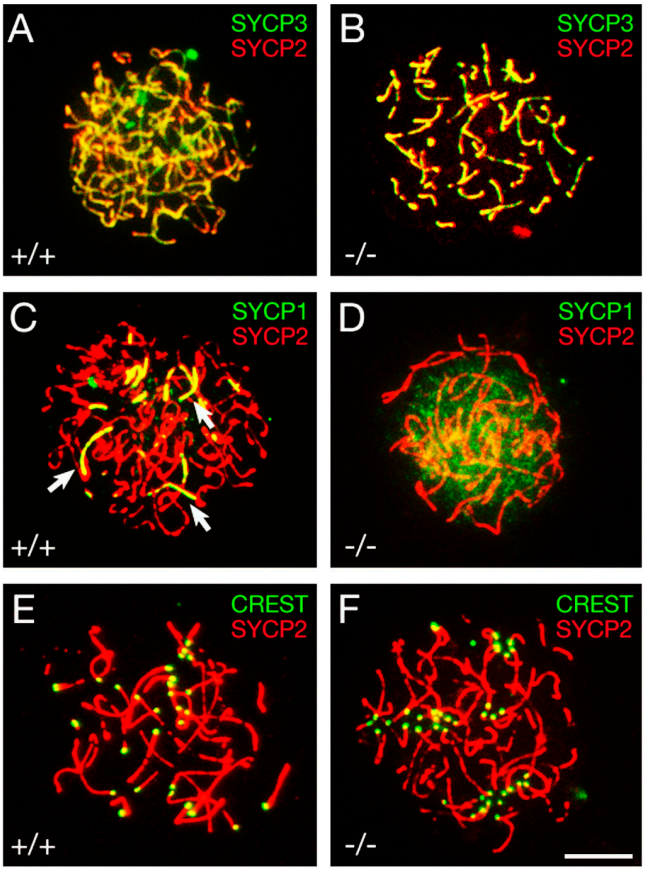

Figure 3. **Failure of chromosomal synapsis in *Tex15*$^{-/-}$ spermatocytes.** Spread nuclei of wild-type (A, C, and E) and *Tex15*-deficient (B, D, and F) spermatocytes were stained with anti-SYCP1, 2, and 3 antibodies and CREST antiserum. (A and B) Formation of axial elements in both wild-type and mutant spermatocytes. (C and D) SYCP1 formed long fibers (C, arrows) along synapsed chromosomes in wild-type zygotene spermatocytes, whereas no such long SYCP1 fibers were observed in *Tex15*-deficient spermatocytes (D). (E) Wild-type zygotene spermatocytes. Note the presence of ~30 CREST foci. (F) Advanced *Tex15*-deficient spermatocytes (as judged by formation of axial elements) contained 40 CREST foci. +/+, wild type; −/−, *Tex15*-deficient. Bar, 10 µm.

meiotic arrest in *Tex15*-deficient testes, we stained testis sections with antibodies against histone H1t, which appears first in mid-to-late pachytene spermatocytes and persists in spermatids (Cobb et al., 1999). *Tex15*-deficient testis lacked H1t-positive cells, suggesting that meiosis is arrested before the midpachytene stage (Fig. S1, available at http://www.jcb.org/cgi/content/full/jcb.200709057/DC1). Histological analysis of juvenile *Tex15*$^{-/-}$ testes also revealed meiotic arrest in the first wave of spermatogenesis (unpublished data). We conclude that *Tex15* is essential for male meiosis and thus required for male fertility.

Tex15 is essential for chromosome synapsis in males

To determine the cause of meiotic arrest in *Tex15*-deficient testes, we examined the assembly of the synaptonemal complex (SC). SYCP2 and 3 are integral components of the axial/lateral elements of the SCs (Fig. 3 A; Dobson et al., 1994; Offenberg et al., 1998; Schalk et al., 1998). Immunostaining of spread spermatocyte nuclei showed that SYCP2 and 3 assembled into axial elements in *Tex15*-deficient spermatocytes (Fig. 3 B). We then assessed the process of synapsis by immunostaining with anti-SYCP1 antibodies. SYCP1, a component of transverse filaments, localizes to the synapsed regions of SC in wild-type zygotene spermatocytes (Fig. 3 C; Dobson et al., 1994; de Vries et al., 2005). However, the majority of advanced *Tex15*$^{-/-}$ spermatocytes did not show any fiber-like SYCP1 staining (Fig. 3 D), whereas only 4% contained a few extremely short stretches of SYCP1 staining. These data demonstrate that *Tex15* is required for chromosomal synapsis during male meiosis.

To validate the synaptic failure observed in *Tex15*-deficient spermatocytes, we analyzed synapsis at centromeric regions by staining with CREST antiserum (Brenner et al., 1981). At the leptotene stage, the maximum number of centromeres (CREST foci) is 40. As chromosomal synapsis progresses from zygotene (Fig. 3 E) to pachytene, the number of CREST foci decreases to 21. We analyzed the number of CREST foci in advanced *Tex15*-deficient spermatocytes in which axial elements were assembled (Fig. 3 F). For the most part, such mutant spermatocytes had 40 foci (39.3 ± 1 CREST foci per nucleus), suggesting that homologous chromosomes failed to undergo synapsis, at least in the centromeric regions (Fig. 3 F). We did not observe cells with >40 CREST foci, suggesting that sister

chromatid cohesion at the centromeric regions is not defective in *Tex15*-deficient spermatocytes.

DSBs are formed, but not repaired, in *Tex15*-deficient males

We then attempted to address whether the synaptic failure in *Tex15*-deficient spermatocytes is caused by impaired meiotic recombination because generation of DSBs by SPO11 and repair of DSBs are required for chromosomal synapsis during meiosis of most organisms including mammals (Zickler and Kleckner, 1999; Keeney, 2001). In mouse, SPO11 generates ~300 DSBs per leptotene nucleus (Keeney, 2001). Formation of DSBs results in the phosphorylation of γH2AX in chromatin (Fig. 4 A). As meiosis proceeds to the pachytene stage, γH2AX disappears from synapsed autosomal chromatin and remains confined to the largely asynapsed sex chromosomes in the XY body (Mahadevaiah et al., 2001). Strikingly, *Tex15*$^{-/-}$ leptotene spermatocytes exhibited intense γH2AX staining throughout the nucleus (Fig. 4 B) and this staining persisted in the most advanced zygotene-like mutant spermatocytes (not depicted). This result suggests that DSBs are formed, but not repaired, and that synaptic failure is likely attributed to defective meiotic recombination in *Tex15*-deficient spermatocytes.

We next monitored the recombination process to address why DSBs are not repaired in *Tex15*$^{-/-}$ spermatocytes. During meiotic recombination, RAD51 and DMC1 are loaded onto sites of DSBs and strand invasion initiates homologue search (Hunter and Kleckner, 2001). In *Tex15*-deficient leptotene and zygotene spermatocytes, the number of RAD51 foci was greatly reduced in comparison with the wild type (Fig. 4, C–E). Greater than 90% of wild-type early spermatocytes contained ~100–250 RAD51 foci (Fig. 4 C). In contrast, >80% of *Tex15*-deficient spermatocytes had no or only a few RAD51 foci (Fig. 4 D). DMC1 is a meiosis-specific homologue of RAD51, and RAD51 and DMC1 colocalize to meiotic chromosomes during meiosis (Tarsounas et al., 1999). A large number of DMC1 foci were present in wild-type zygotene spermatocytes (Fig. 4 F), whereas DMC1 foci were not or were rarely observed in *Tex15*-deficient spermatocytes (Fig. 4 G). Western blot analysis showed that RAD51 and DMC1 were expressed in *Tex15*$^{-/-}$ testes (unpublished data), suggesting that RAD51 and DMC1 are expressed but fail to assemble onto chromatin DSBs. It is unlikely that the dramatically reduced number of RAD51 foci in *Tex15*-deficient spermatocytes is caused by the absence of DMC1 foci because DMC1 is not required for localization of RAD51 to meiotic chromosomes (Pittman et al., 1998; Yoshida et al., 1998). However, it is not known whether RAD51 is required for DMC1 localization because disruption of *Rad51* causes embryonic lethality (Lim and Hasty, 1996; Tsuzuki et al., 1996). Therefore, the lack of DMC1 foci in *Tex15*-deficient spermatocytes could be caused by either the absence of TEX15 or the reduced number of RAD51 foci.

We next examined the localization of replication protein A (RPA). RPA, a ssDNA binding protein, interacts with RAD51 and promotes formation of RAD51 filaments in vitro (Golub et al., 1998). Cytologically, RPA forms foci on synapsed regions of meiotic chromosomes at the zygotene (Fig. 4 H) and, thus, RPA

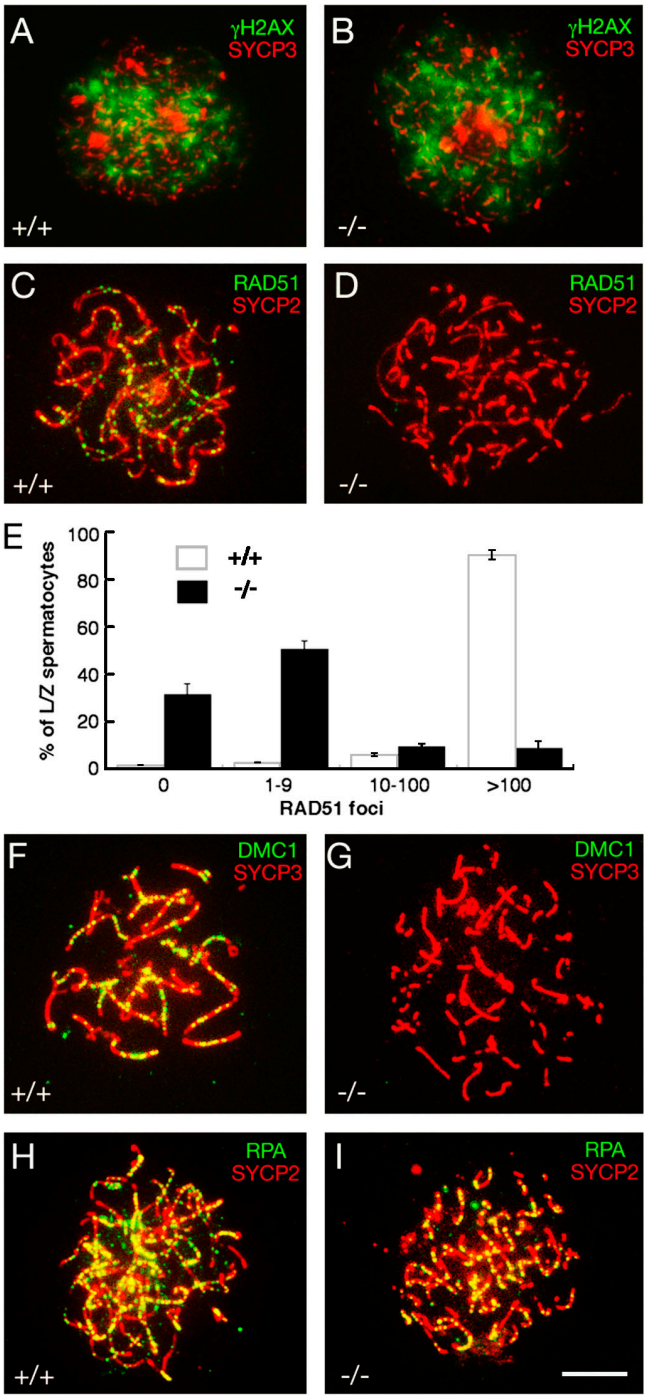

Figure 4. **Meiotic DSBs are generated, but not repaired, in *Tex15*$^{-/-}$ spermatocytes.** Surface-spread nuclei of wild-type and *Tex15*$^{-/-}$ spermatocytes were immunostained with anti-γH2AX, -RAD51, -DMC1, and -RPA antibodies. Axial elements of SCs were labeled with either anti-SYCP2 or anti-SYCP3 antibodies. (A and B) γH2AX is abundant in both wild-type and *Tex15*$^{-/-}$ leptotene spermatocytes. (C–E) Absence or reduction of RAD51 foci in *Tex15*$^{-/-}$ spermatocytes. (E) A dramatic reduction in the number of RAD51 foci per leptotene/zygotene spermatocyte in *Tex15*$^{-/-}$ testes. Values shown represent the mean ± SEM. (F and G) Absence of DMC1 foci in *Tex15*$^{-/-}$ spermatocytes. (H and I) *Tex15*$^{-/-}$ spermatocytes exhibit abundant RPA foci. (C, F, and H) wild-type zygotene spermatocytes; (D, G, and I) advanced *Tex15*$^{-/-}$ spermatocytes. Bar, 10 μm.

foci appear somewhat later than RAD51 and DMC1 foci during meiosis (Plug et al., 1997, 1998; Moens et al., 2002). Intriguingly, despite synaptic failure and a sharply reduced number of RAD51 and DMC1 foci, RPA foci were abundant in *Tex15*$^{-/-}$ spermatocytes (Fig. 4 I). Our study, therefore, suggests that neither TEX15 nor the RAD51–DMC1 complex is required for localization of RPA to meiotic chromosomal cores. It is very intriguing that RPA foci are present even though RAD51 and DMC1 foci are missing in *Tex15*-deficient (this study) or *Brca2* mutant spermatocytes (Sharan et al., 2004). Although cytological appearance of RPA in normal meiosis occurs only after RAD51 and DMC1 dissociate from recombination intermediates, RPA may coat ssDNA before the binding of RAD51 and DMC1 (Bannister and Schimenti, 2004; Marcon and Moens, 2005). This initial binding of RPA to ssDNA on the ends of DSBs is likely too transient to be detectable by cytological analysis because RPA becomes rapidly displaced by the binding of RAD51 and/or DMC1. It is only the binding of RPA to later recombination structures that is visible cytologically. If the loading of RAD51 and DMC1 is defective, the RPA that was initially bound to DSB ends might not be displaced. Thus, the pattern seen in *Tex15* or *Brca2* mutant spermatocytes may reflect the persistence of the initial transient RPA–ssDNA complex in mice.

Tex15-deficient females are fertile

In contrast to the sterility of *Tex15*$^{-/-}$ males, *Tex15*$^{-/-}$ females are fertile, with normal litter size compared with that of wild-type littermate controls. Immunostaining with anti-SYCP1 and -SYCP2 antibodies showed that the assembly of SCs and chromosomal synapsis appears normal in *Tex15*$^{-/-}$ pachytene oocytes (Fig. S2 A, available at http://www.jcb.org/cgi/content/full/jcb.200709057/DC1). We also did not detect a reduction in the number of either RAD51 or DMC1 foci in *Tex15*$^{-/-}$ fetal oocytes compared with the wild type (Fig. S2, B and C). We thus conclude that TEX15 is dispensable for female meiosis. The *Tex15* mutant joins a growing number of mouse mutants with sexual dimorphism of meiotic phenotypes, in that female meiosis is normal or less affected (Hunt and Hassold, 2002). In most, if not all, cases the exact cause of sexual dimorphism is unknown. It has been hypothesized that sexual dimorphism might be attributed to relaxed checkpoint control in females, expedited development of meiosis in females, or the differential behavior of sex chromosomes (Hunt and Hassold, 2002; Kolas et al., 2005). Recently, studies of *Sycp3* and *Dmc1*^{mei11} mutant female mice suggest that fertility might be related to the late activation of the DNA damage checkpoint in females (Wang and Hoog, 2006; Bannister et al., 2007). In this study, the apparently normal loading of RAD51 and DMC1 proteins onto meiotic chromosomes in *Tex15*$^{-/-}$ oocytes could indicate a difference in the recombination pathways between males and females. However, more experiments are required to investigate why meiosis appears to be normal in *Tex15*$^{-/-}$ females.

In summary, we demonstrate that TEX15 is required for meiotic recombination and chromosomal synapsis in males. Our data support a model in which TEX15 functions downstream of the SPO11-mediated DSB formation but upstream of RAD51- and DMC1-mediated DSB repair during the process of meiotic recombination (Fig. 5). Furthermore, the meiotic phenotypes in *Tex15*-deficient mice resemble those observed in mice and rats with mutant BRCA1 or 2 (Xu et al., 2003; Sharan et al., 2004; Cotroneo et al., 2007). BRCA1 is associated with RAD51 (Scully et al., 1997). Although the *Brca1*-null mutation is embryonic lethal, mice carrying a *Brca1* hypomorphic allele (deletion of *Brca1* exon 11) are viable but exhibit a failure in DSB repair during spermatogenesis (Hakem et al., 1998; Xu et al., 2003). BRCA2 binds to RAD51 and regulates its nuclear localization (Davies et al., 2001). Loss of *Brca2* function results in embryonic lethality in mice (Hakem et al., 1998). However, *Brca2*-null mice carrying a human *BRCA2* transgene are viable but defective in meiosis because the human *BRCA2* transgene is poorly expressed in testes and ovaries (Sharan et al., 2004). In this rescued *Brca2* mouse mutant, DSBs are formed but RAD51 and DMC1 fail to assemble into foci on meiotic chromosomes at a wild-type level. A rat strain with a nonsense mutation in exon 11 of *Brca2* is also viable with impaired meiotic recombination (Cotroneo et al., 2007). The similar phenotypes among *Tex15*, *Brca1*, and *Brca2* mutants suggest that TEX15 belongs to a protein family that regulates loading of RAD51 and DMC1 onto sites of DSBs.

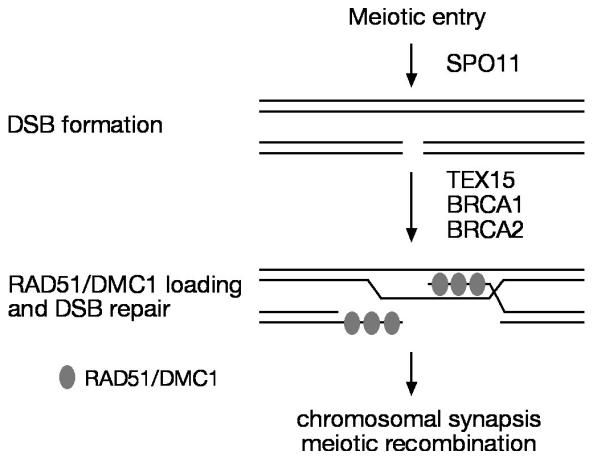

Figure 5. **A model for the role of TEX15 in early meiotic recombination.** Both BRCA1 and 2 interact with RAD51. TEX15, like BRCA1 and 2, apparently functions downstream of SPO11 but upstream of the formation of RAD51 and DMC1 foci at sites of DSBs.

Materials and methods

Generation of anti-TEX15 polyclonal antibodies

The *Tex15* cDNA fragment encoding residues 289–648 was cloned into the pQE-32 vector (QIAGEN). The 6×His-TEX15 (289–648) fusion protein was expressed in M15 bacteria, affinity purified with Ni-NTA beads, and eluted in 8 M urea. The recombinant protein was used to immunize two rabbits (Cocalico Biologicals, Inc). The anti-TEX15 antiserum (serums 2042 and 2043) was used for Western blot (1:200). Specific antibodies were affinity purified with the immunoblot method as previously described (Harlow and Lane, 1998).

Western blotting analyses

Testicular cytoplasmic and nuclear extracts were prepared stepwise using the NE-PER kit according to the manufacturer's protocol (Thermo Fisher Scientific). In brief, adult mouse testes were homogenized in ice-cold CER I buffer. After incubation, ice-cold CER II buffer was added. Samples were spun for 5 min at 16,000 *g*. The supernatant was collected as cytoplasmic extracts. The insoluble fraction was then resuspended in ice-cold NER buffer.

After repeated vortexing and incubations, samples were spun for 10 min at 16,000 *g*. The supernatant (nuclear extract) was collected. 10 µl of each extract was analyzed by SDS-PAGE and Western blot analysis. Western blotting was performed using the following antibodies: anti-TEX15 (1:200), anti-SYCP2 (1:500), anti-SYCP3 (1:2,000), anti-MVH (1:10,000; gift from T. Noce, Mitsubishi Kagaku Institute of Life Sciences, Tokyo, Japan), and anti–β-actin (1:5,000; Sigma-Aldrich).

Targeted inactivation of the *Tex15* gene

Two homologous arms (2.3 and 2.1 kb) were amplified by PCR from a *Tex15*-positive BAC clone (RP23-190F16) and were subcloned to flank the IRES-*LacZ*-PGK-Neo selection cassette (Fig. 1 A; vector is a gift from N.A. Arango and R.R. Behringer, University of Texas M.D. Anderson Cancer Center, Houston, TX). The final targeting construct was fully sequenced, except for the selection cassette, and no PCR mutations were found. Hybrid V6.5 ES cells (C57BL/6 × 129/sv) were electroporated with the linearized *Tex15* targeting construct (pUP32/NotI) and were selected for integration in the presence of 350 µg/ml G418. 384 G418-resistant ES cell clones were screened by PCR for homologous recombination on both sides. Five homologously targeted ES clones were obtained. Two independent clones (2C6 and 3F4) were injected into B6C3F1 blastocysts (Taconic), which were subsequently transferred to uteri of pseudopregnant ICR females. Male chimeras were bred with C57BL/6J females and germ-line transmission of the *Tex15* mutant allele was obtained. No phenotypic difference was observed between mice derived from these two independent ES cell clones. Mice from mixed genetic backgrounds (C57BL/6 × 129/sv) were used in this study. All offspring were genotyped by PCR with the following primers: wild type (542 bp), CTCTGTGAAAGCAATCCAGTG and TCTTCCTCAATGTATTTTGCC; and mutant (300 bp), GTTTATAGGATTCTTTCTCCCT and TCCGATAGCTTGGCTGCAGGTCGACTC. Mice were maintained and used for experimentation according to the guidelines of the Institutional Animal Care and Use Committee of the University of Pennsylvania. According to standard conventions, the *Tex15* knockout allele has been deposited as *Tex15*^{tm1Jw} in the Mouse Genome Informatics database.

Histological, surface-spread, and immunofluorescent analyses

For histology, testes were fixed in Bouin's solution, embedded in paraffin, sectioned, and stained with hematoxylin and eosin. For immunofluorescent analysis, wild-type and *Tex15*-deficient adult testes were fixed in 4% PFA for 3 h at 4°C, dehydrated in 30% sucrose overnight, prepared, sectioned, and double immunostained with rabbit anti-SYCP3 (1:500) and guinea pig anti-H1t antibodies (1:1,000; a gift from M.A. Handel, The Jackson Laboratory, Bar Harbor, ME; Cobb et al., 1999). TUNEL assays were performed with the ApopTag Fluorescein In Situ Apoptosis Detection kit (Millipore).

Surface-spread analysis was performed as previously described (Peters et al., 1997; Kolas et al., 2005). The following primary antibodies were used for immunofluorescence: anti-SYCP1 (gift from C. Heyting, Wageningen University, Wageningen, Netherlands; Schmekel et al., 1996), anti-SYCP2 (1:100; Yang et al., 2006), anti-SYCP3 (1:500; gift from S. Chuma, Kyoto University, Kyoto, Japan; Chuma and Nakatsuji, 2001), human CREST antiserum (1:5,000; gift from B.R. Brinkley, Baylor College of Medicine, Houston, TX; Brenner et al., 1981), anti-γH2AX (1:500; Millipore), rabbit anti-RAD51 (1:20 [BD Biosciences]; or 1:50, H-92 [Santa Cruz Biotechnology, Inc.]), goat anti-DMC1 (1:20, C-20; Santa Cruz Biotechnology, Inc.), rabbit anti-RPA serum (1:400; gift from P. Moens and B. Spyropoulos, York University, Toronto, Canada; Moens et al., 2002). Various FITC- or Texas red–conjugated secondary antibodies and antifade mounting medium with DAPI (Vector Laboratories) were used. Slides were visualized at room temperature using a microscope (Axioskop 40; Carl Zeiss, Inc.) with 40× objectives with an aperture of 0.95 (Carl Zeiss, Inc.). Images were taken with a digital camera (Evolution QEi; MediaCybernetics) and processed with ImagePro software (Phase 3 Imaging Systems) and Photoshop (Adobe).

Online supplemental material

Fig. S1 shows the absence of H1t-positive pachytene spermatocytes in *Tex15*-deficient adult testis to demonstrate that the point of meiotic arrest caused by disruption of *Tex15* is before the mid-pachytene stage. Fig. S2 shows the assembly of SCs and the distribution of RAD51 and DMC1 in *Tex15*$^{-/-}$ fetal oocytes. Online supplemental material is available at http://www.jcb.org/cgi/content/full/jcb.200709057/DC1.

We thank P. Moens and B. Spyropoulos for anti-RPA antibodies, M.A. Handel for anti-H1t antibodies, C. Heyting for anti-SYCP1 antibodies, S. Chuma for anti-SYCP3 antibodies, B.R. Brinkley for CREST, T. Noce for anti-MVH antibodies, and N.A. Arango and R.R. Behringer for the PGK-neo vector.

This work was supported by the University of Pennsylvania Research Foundation and a National Institutes of Health/National Institutes of Child Health and Human Development grant (HD 045866).

Submitted: 10 September 2007
Accepted: 24 January 2008

References

Bannister, L.A., and J.C. Schimenti. 2004. Homologous recombinational repair proteins in mouse meiosis. *Cytogenet. Genome Res.* 107:191–200.

Bannister, L.A., R.J. Pezza, J.R. Donaldson, D.G. de Rooij, K.J. Schimenti, R.D. Camerini-Otero, and J.C. Schimenti. 2007. A dominant, recombination-defective allele of Dmc1 causing male-specific sterility. *PLoS Biol.* 5:e105.

Baudat, F., K. Manova, J.P. Yuen, M. Jasin, and S. Keeney. 2000. Chromosome synapsis defects and sexually dimorphic meiotic progression in mice lacking Spo11. *Mol. Cell.* 6:989–998.

Bishop, D.K., D. Park, L. Xu, and N. Kleckner. 1992. DMC1: A meiosis-specific yeast homolog of *E. coli* recA required for recombination, synaptonemal complex formation, and cell cycle progression. *Cell.* 69:439–456.

Brenner, S., D. Pepper, M.W. Berns, E. Tan, and B.R. Brinkley. 1981. Kinetochore structure, duplication, and distribution in mammalian cells: analysis by human autoantibodies from scleroderma patients. *J. Cell Biol.* 91:95–102.

Chuma, S., and N. Nakatsuji. 2001. Autonomous transition into meiosis of mouse fetal germ cells in vitro and its inhibition by gp130-mediated signaling. *Dev. Biol.* 229:468–479.

Cobb, J., B. Cargile, and M.A. Handel. 1999. Acquisition of competence to condense metaphase I chromosomes during spermatogenesis. *Dev. Biol.* 205:49–64.

Cotroneo, M.S., J.D. Haag, Y. Zan, C.C. Lopez, P. Thuwajit, G.V. Petukhova, R.D. Camerini-Otero, A. Gendron-Fitzpatrick, A.E. Griep, C.J. Murphy, et al. 2007. Characterizing a rat *Brca2* knockout model. *Oncogene.* 26:1626–1635.

Davies, A.A., J.Y. Masson, M.J. McIlwraith, A.Z. Stasiak, A. Stasiak, A.R. Venkitaraman, and S.C. West. 2001. Role of BRCA2 in control of the RAD51 recombination and DNA repair protein. *Mol. Cell.* 7:273–282.

de Vries, F.A., E. de Boer, M. van den Bosch, W.M. Baarends, M. Ooms, L. Yuan, J.G. Liu, A.A. van Zeeland, C. Heyting, and A. Pastink. 2005. Mouse *Sycp1* functions in synaptonemal complex assembly, meiotic recombination, and XY body formation. *Genes Dev.* 19:1376–1389.

Dobson, M.J., R.E. Pearlman, A. Karaiskakis, B. Spyropoulos, and P.B. Moens. 1994. Synaptonemal complex proteins: occurrence, epitope mapping and chromosome disjunction. *J. Cell Sci.* 107:2749–2760.

Golub, E.I., R.C. Gupta, T. Haaf, M.S. Wold, and C.M. Radding. 1998. Interaction of human rad51 recombination protein with single-stranded DNA binding protein, RPA. *Nucleic Acids Res.* 26:5388–5393.

Hakem, R., J.L. de la Pompa, and T.W. Mak. 1998. Developmental studies of *Brca1* and *Brca2* knock-out mice. *J. Mammary Gland Biol. Neoplasia.* 3:431–445.

Harlow, E., and D. Lane. 1998. Using Antibodies: a Laboratory Manual. Cold Spring Harbor Laboratory Press, Cold Spring Harbor, NY. 481 pp.

Hunt, P.A., and E.M. Eicher. 1991. Fertile male mice with three sex chromosomes: evidence that infertility in XYY male mice is an effect of two Y chromosomes. *Chromosoma.* 100:293–299.

Hunt, P.A., and T.J. Hassold. 2002. Sex matters in meiosis. *Science.* 296:2181–2183.

Hunter, N., and N. Kleckner. 2001. The single-end invasion: an asymmetric intermediate at the double-strand break to double-holliday junction transition of meiotic recombination. *Cell.* 106:59–70.

Keeney, S. 2001. Mechanism and control of meiotic recombination initiation. *Curr. Top. Dev. Biol.* 52:1–53.

Keeney, S., C.N. Giroux, and N. Kleckner. 1997. Meiosis-specific DNA double-strand breaks are catalyzed by Spo11, a member of a widely conserved protein family. *Cell.* 88:375–384.

Kolas, N.K., E. Marcon, M.A. Crackower, C. Hoog, J.M. Penninger, B. Spyropoulos, and P.B. Moens. 2005. Mutant meiotic chromosome core components in mice can cause apparent sexual dimorphic endpoints at prophase or X-Y defective male-specific sterility. *Chromosoma.* 114:92–102.

Libby, B.J., L.G. Reinholdt, and J.C. Schimenti. 2003. Positional cloning and characterization of Mei1, a vertebrate-specific gene required for normal meiotic chromosome synapsis in mice. *Proc. Natl. Acad. Sci. USA.* 100:15706–15711.

Lim, D.S., and P. Hasty. 1996. A mutation in mouse rad51 results in an early embryonic lethal that is suppressed by a mutation in p53. *Mol. Cell. Biol.* 16:7133–7143.

Mahadevaiah, S.K., J.M. Turner, F. Baudat, E.P. Rogakou, P. de Boer, J. Blanco-Rodriguez, M. Jasin, S. Keeney, W.M. Bonner, and P.S. Burgoyne. 2001. Recombinational DNA double-strand breaks in mice precede synapsis. *Nat. Genet.* 27:271–276.

Marcon, E., and P.B. Moens. 2005. The evolution of meiosis: recruitment and modification of somatic DNA-repair proteins. *Bioessays.* 27:795–808.

Moens, P.B., N.K. Kolas, M. Tarsounas, E. Marcon, P.E. Cohen, and B. Spyropoulos. 2002. The time course and chromosomal localization of recombination-related proteins at meiosis in the mouse are compatible with models that can resolve the early DNA-DNA interactions without reciprocal recombination. *J. Cell Sci.* 115:1611–1622.

Offenberg, H.H., J.A. Schalk, R.L. Meuwissen, M. van Aalderen, H.A. Kester, A.J. Dietrich, and C. Heyting. 1998. SCP2: A major protein component of the axial elements of synaptonemal complexes of the rat. *Nucleic Acids Res.* 26:2572–2579.

Peters, A.H., A.W. Plug, M.J. van Vugt, and P. de Boer. 1997. A drying-down technique for the spreading of mammalian meiocytes from the male and female germline. *Chromosome Res.* 5:66–68.

Pittman, D.L., J. Cobb, K.J. Schimenti, L.A. Wilson, D.M. Cooper, E. Brignull, M.A. Handel, and J.C. Schimenti. 1998. Meiotic prophase arrest with failure of chromosome synapsis in mice deficient for *Dmc1*, a germline-specific RecA homolog. *Mol. Cell.* 1:697–705.

Plug, A.W., A.H. Peters, Y. Xu, K.S. Keegan, M.F. Hoekstra, D. Baltimore, P. de Boer, and T. Ashley. 1997. ATM and RPA in meiotic chromosome synapsis and recombination. *Nat. Genet.* 17:457–461.

Plug, A.W., A.H. Peters, K.S. Keegan, M.F. Hoekstra, P. de Boer, and T. Ashley. 1998. Changes in protein composition of meiotic nodules during mammalian meiosis. *J. Cell Sci.* 111:413–423.

Romanienko, P.J., and R.D. Camerini-Otero. 2000. The mouse *Spo11* gene is required for meiotic chromosome synapsis. *Mol. Cell.* 6:975–987.

Schalk, J.A., A.J. Dietrich, A.C. Vink, H.H. Offenberg, M. van Aalderen, and C. Heyting. 1998. Localization of SCP2 and SCP3 protein molecules within synaptonemal complexes of the rat. *Chromosoma.* 107:540–548.

Schmekel, K., R.L. Meuwissen, A.J. Dietrich, A.C. Vink, J. van Marle, H. van Veen, and C. Heyting. 1996. Organization of SCP1 protein molecules within synaptonemal complexes of the rat. *Exp. Cell Res.* 226:20–30.

Scully, R., J. Chen, A. Plug, Y. Xiao, D. Weaver, J. Feunteun, T. Ashley, and D.M. Livingston. 1997. Association of BRCA1 with Rad51 in mitotic and meiotic cells. *Cell.* 88:265–275.

Sharan, S.K., A. Pyle, V. Coppola, J. Babus, S. Swaminathan, J. Benedict, D. Swing, B.K. Martin, L. Tessarollo, J.P. Evans, et al. 2004. BRCA2 deficiency in mice leads to meiotic impairment and infertility. *Development.* 131:131–142.

Tarsounas, M., T. Morita, R.E. Pearlman, and P.B. Moens. 1999. RAD51 and DMC1 form mixed complexes associated with mouse meiotic chromosome cores and synaptonemal complexes. *J. Cell Biol.* 147:207–220.

Toyooka, Y., N. Tsunekawa, Y. Takahashi, Y. Matsui, M. Satoh, and T. Noce. 2000. Expression and intracellular localization of mouse vasa-homologue protein during germ cell development. *Mech. Dev.* 93:139–149.

Tsuzuki, T., Y. Fujii, K. Sakumi, Y. Tominaga, K. Nakao, M. Sekiguchi, A. Matsushiro, Y. Yoshimura, and T. Morita. 1996. Targeted disruption of the *Rad51* gene leads to lethality in embryonic mice. *Proc. Natl. Acad. Sci. USA.* 93:6236–6240.

Wang, H., and C. Hoog. 2006. Structural damage to meiotic chromosomes impairs DNA recombination and checkpoint control in mammalian oocytes. *J. Cell Biol.* 173:485–495.

Wang, P.J., and J. Pan. 2007. The role of spermatogonially expressed germ cell-specific genes in mammalian meiosis. *Chromosome Res.* 15:623–632.

Wang, P.J., J.R. McCarrey, F. Yang, and D.C. Page. 2001. An abundance of X-linked genes expressed in spermatogonia. *Nat. Genet.* 27:422–426.

Wang, P.J., D.C. Page, and J.R. McCarrey. 2005. Differential expression of sex-linked and autosomal germ-cell-specific genes during spermatogenesis in the mouse. *Hum. Mol. Genet.* 14:2911–2918.

Xu, X., O. Aprelikova, P. Moens, C.X. Deng, and P.A. Furth. 2003. Impaired meiotic DNA-damage repair and lack of crossing-over during spermatogenesis in BRCA1 full-length isoform deficient mice. *Development.* 130:2001–2012.

Yang, F., R. De La Fuente, N.A. Leu, C. Baumann, K.J. McLaughlin, and P.J. Wang. 2006. Mouse SYCP2 is required for synaptonemal complex assembly and chromosomal synapsis during male meiosis. *J. Cell Biol.* 173:497–507.

Yoshida, K., G. Kondoh, Y. Matsuda, T. Habu, Y. Nishimune, and T. Morita. 1998. The mouse RecA-like gene *Dmc1* is required for homologous chromosome synapsis during meiosis. *Mol. Cell.* 1:707–718.

Zickler, D., and N. Kleckner. 1999. Meiotic chromosomes: integrating structure and function. *Annu. Rev. Genet.* 33:603–754.